J. Microbiol. Biotechnol. (2017), 27(6), 1150–1156
https://doi.org/10.4014/jmb.1701.01060

jmb

Highly Time-Resolved Metabolic Reprogramming toward Differential Levels of Phosphate in *Chlamydomonas reinhardtii*

Cheol-Ho Jang[1†], Gayeon Lee[1†], Yong-Cheol Park[1], Kyoung Heon Kim[2], and Do Yup Lee[1*]

[1]*Depatment of Bio and Fermentation Convergence Technology, BK21 PLUS Program, Kookmin University, Seoul 02707, Republic of Korea*
[2]*Depatment of Biotechnology, Graduate School, Korea University, Seoul 02841, Republic of Korea*

Received: January 24, 2017
Revised: March 29, 2017
Accepted: March 30, 2017

First published online
April 3, 2017

**Corresponding author*
Phone: +82-2-910-5733;
Fax: +82-2-910-5733;
E-mail: rome73@kookmin.ac.kr

†These authors contributed equally to this work.

Supplementary data for this paper are available on-line only at http://jmb.or.kr.

pISSN 1017-7825, eISSN 1738-8872

Understanding phosphorus metabolism in photosynthetic organisms is important as it is closely associated with enhanced crop productivity and pollution management for natural ecosystems (*e.g.*, algal blooming). Accordingly, we exploited highly time-resolved metabolic responses to different levels of phosphate deprivation in *Chlamydomonas reinhardtii*, a photosynthetic model organism. We conducted non-targeted primary metabolite profiling using gas-chromatography time-of-flight mass spectrometric analysis. Primarily, we systematically identified main contributors to degree-wise responses corresponding to the levels of phosphate deprivation. Additionally, we systematically characterized the metabolite sets specific to different phosphate conditions and their interactions with culture time. Among them were various types of fatty acids that were most dynamically modulated by the phosphate availability and culture time in addition to phosphorylated compounds.

Keywords: *Chlamydomonas reinhardtii*, GC-TOF MS, phosphorus, temporal resolution, dose responsiveness

Introduction

Phosphorus (P) is an essential macronutrient for growth and production in all living organisms, including such photosynthetic organisms as higher plants and photosynthetic microalgae [1, 2]. Primarily, phosphorus composes structural constituents (*e.g.*, nucleic acids and phospholipids), and universally altered carbohydrates and proteins [2]. Thus, phosphorus deprivation provokes complicated metabolic reshuffling, which allows scavenging and relocation processes for phosphorus coupled with photosynthetic carbon fixation and carbohydrate-nitrogen metabolism [3]. Since the nutrient is frequently limited owing to relatively high demands and frequent sequestration as unavailable chemical forms [4], comprehensive studies on phosphorus metabolism lead to better agricultural and environmental strategies by optimizing the management and development of more suitable crops [5].

However, investigations using higher plant systems are often complicated by long development periods and the existence of multiple cell types, which all obstruct the comprehensive understanding of the highly interactive regulatory processes involved in metabolism [6]. Alternatively, the unicellular green alga *Chlamydomonas reinhardtii* is an attractive resource as a model organism, as it has been fully genome-sequenced and is available for genetic and molecular tools. In particular, this organism has been studied for the purpose of resolving the responses of photosynthetic eukaryotes to the deprivation of various nutrients [7, 8], including nitrogen [9–11], sulfur [12–14], phosphorus [2, 4, 15], and iron [16–18].

Accordingly, we exploited the photosynthetic microalga *C. reinhardtii* to systematically characterize metabolic responses to phosphate deprivation. In order to enrich understanding of the intricate metabolic modulation, we applied metabolome-wide analysis using GC-TOF MS

with an emphasis on primary metabolites. In addition to examining a snapshot at a single time point [19], we monitored time-dependent dynamics in metabolic regulation along with five representative growth phases [20]. Furthermore, we conducted degree-wise metabolic responses by applying differential levels of phosphate deprivation, which aids in resolving the factor-specific metabolic features from temporal effects on the metabolism [21].

Materials and Methods

Growth Condition

C. reinhardtii wild-type strain CC125 was used for this study. The cells were cultured in Tris acetate phosphate medium at 23°C under continual illumination with cool-white fluorescent bulbs at a fluence rate of 70 μmol m^{-2} s^{-1} and with continuous shaking (130 rpm) for pre-culture. The pre-culture was harvested at late log-phase and used to inoculate a main culture at a starting density of 5 × 10^6 cells/ml under three different phosphate conditions (control condition with 1 mM-100%, partially deprived condition of 0.5 mM-50%, and completely deprived condition of 0 mM-0%) using a 20 ml total volume in 125 ml flasks. Six independent cultures for each condition were used for metabolite profiling. The cell numbers were counted using the EVE automatic cell counter (NanoEnTek, USA).

Quenching and Extraction Method for Metabolite Profiling

For the quenching step, 1 ml of cell culture was rapidly mixed with 1 ml of −20°C cold methanol (70% methanol in pure water (v/v)) [22]. The quenched cells were collected after centrifugation (5 min at 16,100 ×*g*) at 4°C and prompt removal of the supernatant. The cell pellets were lyophilized (48 h), and stored at −80°C until analysis. The lyophilized cells were ground using a single 5 mm i.d. steel ball using mixer Mill MM400 (Retsch GmbH & Co., Germany) followed by the addition of 750 μl of extraction solvent (methanol:isopropanol:water, 3:3:2 (v/v/v)) [23]. Afterwards, the mixtures were sonicated (5 min), centrifuged (5 min, 16,100 ×*g* at 4°C), and transferred to a new 1.5 ml tube. The aliquots were concentrated to complete dryness.

GC-TOF MS Analysis

Five microliters of pyridine (Thermo, USA) with 40 mg/ml methoxyamine hydrochloride (Sigma-Aldrich, USA) was added to the dried extracts and incubated (200 rpm and 90 min at 30°C) for the first derivatization step. Two microliters of fatty acid methyl esters (FAMEs) and 45 μl of *N*-methyl-*N*-trimethylsilyltrifluoroacetamide (MSTFA + 1% TMCS; Thermo, USA) were added, and shaken for 60 min (200 rpm at 37°C). The derivatized metabolites were injected using an Agilent 7890B ALS (Agilent, USA) in splitless mode, chromatographically separated on the Agilent 7890B gas chromatograph, and analyzed with a LECO Pegasus HT time-of-flight mass spectrometer [24].

Data Processing and Statistical Analysis

Result files were exported to a server computer and processed by the BinBase algorithm [25]. The processed raw data were then normalized by total ion chromatogram signals of all structurally identified compounds before statistical analysis.

Univariate statistical analyses were conducted with the Student's *t*-test ($p < 0.05$) using the Statistica software ver. 7.0 (StatSoft, USA). The score scatter plot, loading scatter plot, variable importance in projection analysis, and shared-unique structure plot analysis were carried out using by orthogonal projections to latent structures-discriminant analysis (O2PLS-DA) using SIMCA-P (ver. 14.0; Umetrics, Sweden). ANOVA-simultaneous component analysis (ASCA) was performed with the dataset, with log-transformation and auto-scaling implemented in the Metaboanalyst web portal [26].

Results and Discussion

Alterations in Cellular Growth and Metabolic Phenotype in Response to Phosphate Deprivation

Differential cellular growth was observed after 48 h under the 0%-P condition ($p = 0.038$), whereas the 50%-P condition did not show significant differences ($p = 0.542$) after 96-h culture compared with the control (Fig. 1). Subsequently, we selected five different time points (8, 12, 24, 48, and 96 h) to monitor the metabolic responses of the *Chlamydomonas* cells to differential levels of phosphate deficiency. We applied non-targeted metabolite profiling based on GC-TOF MS which resulted in the structural identification of 83 compounds with 1,061 metabolic signatures using the BinBase algorithm. A list of all identified metabolites is provided in Supplemental Fig. S1.

Initially, orthogonal partial least squares discriminant analysis (O2PLS-DA) revealed that the metabolic phenotype

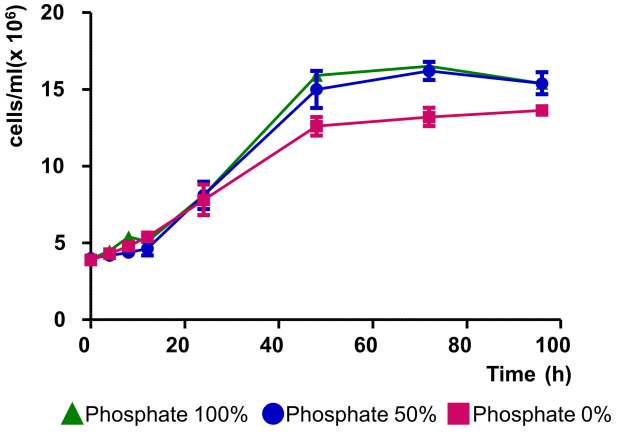

Fig. 1. Cell growth curves under the control (100%-P), 50%-P, and 0%-P conditions ($n = 6$ for each).

was primarily influenced by culture time, where the metabolite profiles showed transitional changes in a counterclockwise direction in the score scatter plot (Fig. 2A). Different levels of phosphate content also induced distinctive metabolic regulation, which was amplified with culture time (Fig. 2A). Despite the identical growth rates, the cells in the 50%-P condition showed distinct clusters from those in 100%-P at all time points (R^2Y = 0.851 and Q^2 = 0.571) (Fig. S2), when the two conditions were directly compared.

Major contributors to the distinctive metabolic regulation in a time-dependent manner were identified using variable importance plot analysis. Primarily, phosphate-containing metabolites were at the top of the list, which included phosphate, pyrophosphate, fructose-6-phosphate, 6-phosphogluconic acid, and glucose-6-phosphate (Fig. 2B). The exclusive alteration in phosphorylated compounds was in accordance with observations in higher plant systems such as barley [27] and maize [28]. The rest of the list was amino acids, homoserine, β-alanine, nucleosides, 5′-deoxy-5′-methylthioadenosine, and guanosine. Homoserine, an intermediate for methionine, threonine, and isoleucine biosynthesis, has been reported to be an important constituent of the ether lipid complex in *C. reinhardtii* [29]. The association with altered lipid metabolism was also found in increased levels in beta-alanine, which is converted to malonyl-CoA and enters fatty acid biosynthesis. The characteristic changes in the amino acids linked to lipid metabolism were evidenced by the concomitant up-regulation in a broad range of fatty acids in the phosphate-deprived cells (Fig. S3). In addition to the changes in the specific amino acids linked to lipid metabolism, a range of amino acids showed significant increases in their contents, especially at 96 h (Fig. S3). The concomitant increases in general amino acids implied an up-regulation in the protein digestion process triggered by nutritional deficiency [28]. The increased amino acid levels in *Chlamydomonas* cells were consistent with previous reports on maize [28]. Likewise, proteomics analysis of a marine diatom, *Phaeodactylum tricornutum*, revealed up-regulation in the metabolic process under phosphorus deprivation [30].

Systematic Isolation of the Phosphate Condition-Specific Metabolic Response

The temporal effect veiled the differential metabolic phenotypes of the *Chlamydomonas* cells under P-deprivation conditions, as seen in the sample score scatter plot (Fig. 2). Thus, we explored the isolation metabolite sets whose regulation was exclusively dependent on the phosphate

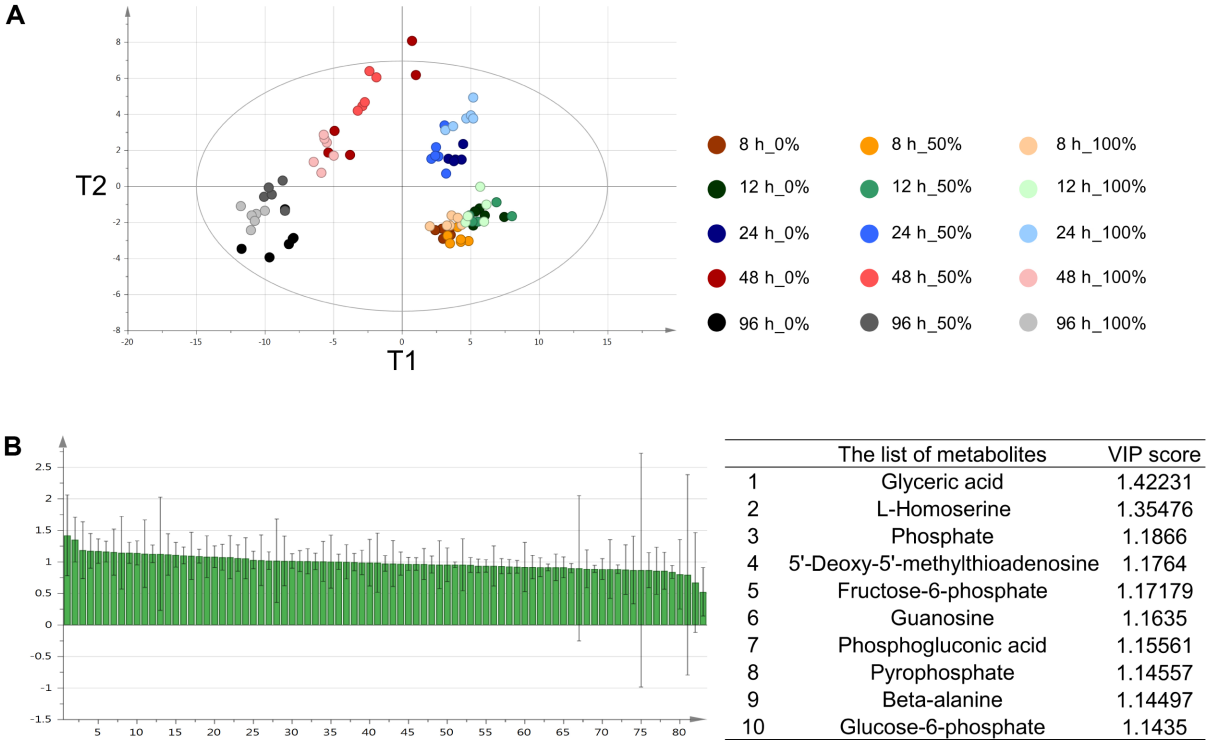

	The list of metabolites	VIP score
1	Glyceric acid	1.42231
2	L-Homoserine	1.35476
3	Phosphate	1.1866
4	5'-Deoxy-5'-methylthioadenosine	1.1764
5	Fructose-6-phosphate	1.17179
6	Guanosine	1.1635
7	Phosphogluconic acid	1.15561
8	Pyrophosphate	1.14557
9	Beta-alanine	1.14497
10	Glucose-6-phosphate	1.1435

Fig. 2. (**A**) The score scatter plot, and (**B**) the plot of variable importance in projection (VIP) analysis and the list of metabolites with the highest VIP scores analyzed by orthogonal projection to latent structures-discriminant analysis (O2PLS-DA).

availability. In order to systematically resolve phosphate condition-specific metabolite dynamics from the time dimension, we performed the ASCA. This statistical method splits variations of the entire dataset into parts that can be allocated to influences from different factors and their interactions [31, 32]. The ASCA was first conducted to construct well-modeled components that corresponded to the phosphate condition, culture time, or an interaction between the two factors. The statistical power was evaluated with a permutation test (20 times), which resulted in validation of the model as confirmed by the statistical values $p = 0.05$, $p < 0.05$, and $p = 0.3$ for culture condition, time, and interaction, respectively (Fig. S4). The resultant model isolated major trends associated with culture condition and time. The condition-specific pattern was primarily characterized by gradual decreases according to the phosphate levels (Fig. S4). Subsequent analysis revealed that the significant factors were phosphate, glyceric acid, lignoceric acid, 2-hydroxypyridine, glycerol-1-phosphate, and phosphogluconic acid (Fig. 3A). In addition, the metabolites, which were designated as interactive factors with a combination of culture condition and time, were mainly free fatty acids such as palmitic acid, stearic acid, pentadecanoic acid, heptadecanoic acid, and oleic acid (Fig. 3B). The fatty acids showed interactive expression levels, with characteristic temporal patterns as the phosphate level decreased (Fig. S5). The metabolites under the control condition were relatively constant or decreased moderately with increased culture duration, whereas those at 50%-P reached maximum abundance at 12 h and gradually decreased afterward. Likewise, the fatty acids at 0%-P showed similar temporal alterations but the expression levels reached the highest levels with the longest culture period (96 h).

Metabolic Commonness and Uniqueness between Different Levels of Phosphate Availability

Next, we explored the primary factors that correspond to (i) common metabolic responses shared by 50%-P and 0%-P conditions and (ii) unique metabolic regulation distinctively induced by each condition. In order to systematically identify the different types of metabolite sets, we applied a statistical approach using shared-and-unique-structures plot analysis in the O2PLS-DA model [33, 34]. The metabolites distributed along the diagonal line indicated a similar pattern of metabolic regulation between the two

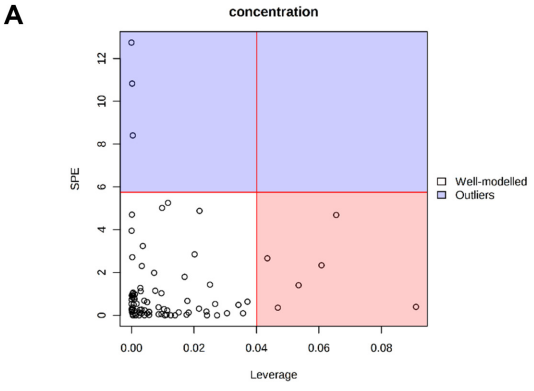

Name	Kegg ID	Leverage	SPE
Phosphate	C00009	0.0910678	0.396489
Glyceric acid	C00258	0.0655202	4.68825
Lignoceric acid	C08320	0.0608148	2.33771
2-Hydroxypyridine	C02502	0.0534844	1.40526
Glycerol-1-phosphate	C03189	0.0468443	0.359164
Phosphogluconic acid	C00345	0.043491	2.66461

Name	Kegg ID	Leverage	SPE
Palmitic acid	C00249	0.177209	6.4731
Heptadecanoic acid	N/A	0.106504	1.63222
Stearic acid	C01530	0.104075	7.85898
Pentadecanoic acid	C16537	0.0934713	3.02824
Succinic acid	C00042	0.0911089	1.59392
Oleic acid	C00712	0.0908747	0.995818

Fig. 3. ANOVA-simultaneous component analysis (ASCA) with leverage/squared prediction error (SPE) scatter plots and the significant factors of the ASCA-variables submodel (**A**) culture condition and (**B**) interaction between culture condition and time.

conditions (50 and 0%-P) in a positive or negative direction compared with the control. Likewise the metabolites positioned near the x- and y-axes presented unique effects, which were distinctively regulated by the two different conditions (50 and 0%-P) compared with the control.

O2PLS-DA models were constructed by pairwise comparison of 50%- and 0%- P conditions with the control at each culture time point (8, 12, 24, 48, and 96 h). Primarily, joint metabolic responses between both conditions dominated for most of metabolites across all culture durations (Fig. 4 and Fig. S4). The results showed that similar patterns of metabolic responses were provoked by phosphate deficiency, regardless of the level. A few exceptions were detected at 8, 12, and 96 h. Medium-chain fatty acids (MFAs), pelargonic acid (C9:0), capric acid (C10:0), and lauric acid (C10:0) showed up-regulation in 0%-P, but they were down-regulated under 50%-P relative to the controls. The opposite expression patterns were sustained during the early time points (8 and 12 h). Contrarily, long-chain fatty acids (LFAs) and neutral lipids were up-regulated exclusively in 50%-P at equivalent time points. These LFAs included palmitic acid (C16:0), linolenic acid (C18:3), 1-monopalmitin, and 1-monostearin (Fig. S6).

In contrast, the *Chlamydomonas* cells responded orthogonally according to the levels of phosphate at 24 and 48 h (Fig. 4). The metabolites within boxes 1 and 3 exhibited 0% P-specific alterations in positive or negative directions, whereas those within boxes 2 and 4 showed 50% P-specific regulation. At 24 h, *Chlamydomonas* cells that were partially deprived of phosphate (50%-P) overproduced pyrophosphate, sorbitol, mannitol, linolenic acid, and 2-hydroxyvaleric acid. Increased levels of urea were accompanied by a decrease in cytidine-5-monophosphate and beta-alanine, which were linked to recycling in the pyrimidine pathway. The cells under complete P-deprivation (0%-P) were characterized by alterations in central carbon and nitrogen metabolisms. In particular, the increase in glucose with the decrease of glucose-6-phosphate indicated a direct impact of P-deprivation on the rate-limiting step of glycolysis. Increased levels of glycerate also implied a slow-down in central carbon metabolism where glycerate is converted to glycerate-2-phosphate or glycerate-3-phosphate via phosphorylation. After 48 h, down-regulation of free fatty acids with longer chain lengths, such as myristic acid (C14:0), pentadecanoic acid (C15:0), and heptadecanoic acid (C17:0), was prevalent under the phosphate-deprived condition, whereas MFAs showed a negative specific correlation with mild phosphate suppression (50%-P).

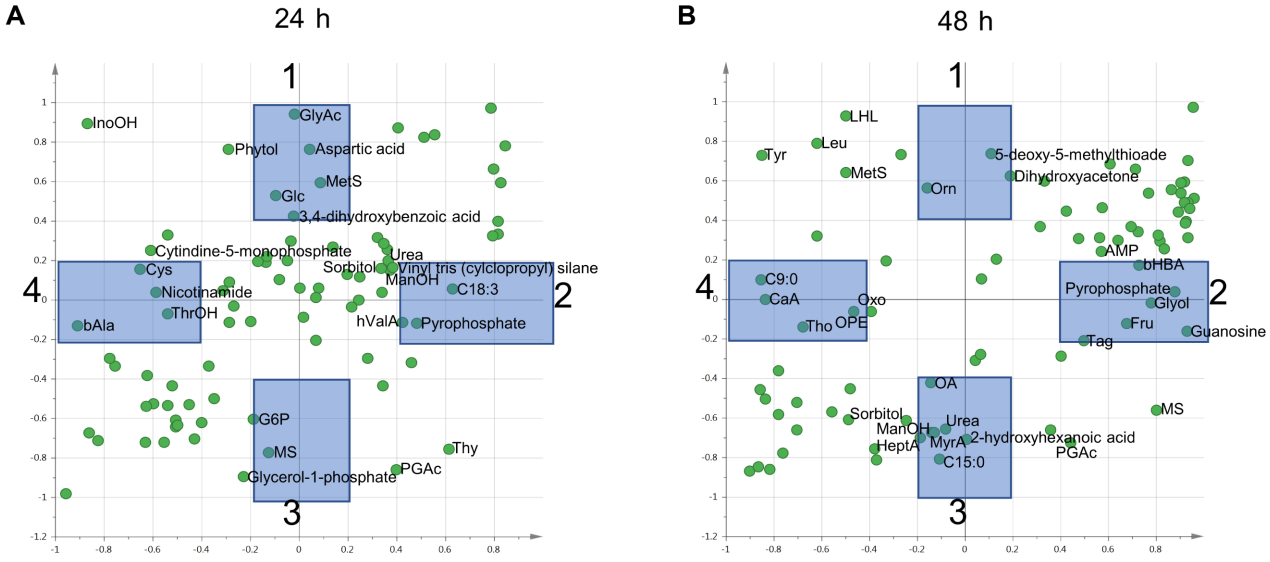

Fig. 4. Shared-unique structure plot analysis by O2PLS-DA.

The x-axis presents the model discriminating between the control versus 50%-P and the y-axis indicates the separating model for the comparison between the control versus 0%-P at the time point of 24 h (**A**) and 48 h (**B**). (**A**) Myo-inositol (InoOH), glyceric acid (GlyAc), methionine sulfoxide (MetS), glucose (Glc), L-cysteine (Cys), threitol (ThrOH), beta-alanine (bAla), mannitol (ManOH), linolenic acid (C18:3), 2-hydroxyvaleric acid (hValA), glucose-6-phospahte (G6P), 1-monostearin (MS), thymine (Thy), and phosphogluconic acid (PGAc). (**B**) L-Homoserine (LHL), leucine (Leu), tyrosine (Tyr), ornithine (Orn), pelargonic acid (C9:0), capric acid (CaA), oxoproline (Oxo), *O*-phosphorylethanolamine (OPE), threose (Tho), adenosine-5-monophosphate (AMP), beta-hydroxybutyric acid (bHBA), glycerol (Glyol), fructose (Fru), tagatose (Tag), oleic acid (OA), myristic acid (MyrA), heptadecanoic acid (HeptA), and pentadecanoic acid (C15:0).

Considering the linkage between the primary metabolism and the integrative cellular physiology, it was interesting that the significant alterations observed in the central carbon metabolism, fatty acid metabolism, and amino acid metabolism in the 50%-P condition were not accompanied by a differential growth rate. The relatively lower level of phosphorus may be sufficient to maintain cellular growth at a rate comparable to 100%-P; however, the suboptimal level may induce differential metabolic regulation as observed in our study. The cells may explore optimal redistribution of biochemical resources by sensitively sensing and rapidly adapting to the continuously changing environmental factors [7, 24].

In addition, we analyzed a potential linkage of the central carbon/nitrogen metabolism, which was globally reshuffled by the phosphate deprivation, to the secondary metabolism. Indeed, preliminary pathway mapping onto the Kyoto Encyclopedia of Genes and Genomes database implied that the long exposure under phosphate deficiency led to an alteration in secondary metabolism (Fig. S7). The potential activation of secondary metabolism was predicted on the basis of increased levels of amino acids and organic acids. The up-regulation of tyrosine, valine, isoleucine, leucine, succinate, citrate, and fumarate was linked to the potential activation of alkaloid biosynthesis [35]. Tyrosine, valine, isoleucine, and leucine were linked to the biosynthesis of glucosinolate, whereas the increased levels of succinate, citrate, and fumarate indicated the up-regulated biosynthesis of phenylpropanoids and terpenoids [36]. Although we limited the scope to primary metabolites in the current study, integrative analysis including secondary metabolism and using a compatible analytical platform (*e.g.*, LC-MS) can lead to more comprehensive understanding of the metabolic network in response to nutritional stress in a photosynthetic microalga.

Overall, our findings in the current experiment demonstrated the metabolic sensitivity of the *Chlamydomonas* cells, which is sufficient to respond distinctively to subtle differences in the medium contents (phosphate levels) despite identical physiological properties (*e.g.*, cell growth). Furthermore, the metabolomic profiles consisting of degree-wise perturbation with temporal dynamics revealed culture condition-specific regulation and shared metabolic synchronization, which was successfully resolved from the time-dependent metabolic responses.

Acknowledgments

This research was supported by the National Research Foundation of Korea Grant (2013R1A1A1058163 and 2015M3A6A2065749), and also by the R&D Program of MOTIE/KEIT (10044647) funded by the Ministry of Science, ICT and Future Planning and Technology.

References

1. Calderón-Vázquez C, Sawers RJ, Herrera-Estrella L. 2011. Phosphate deprivation in maize: genetics and genomics. *Plant Physiol.* **156:** 1067-1077.
2. Moseley JL, Gonzalez-Ballester D, Pootakham W, Bailey S, Grossman AR. 2009. Genetic interactions between regulators of *Chlamydomonas* phosphorus and sulfur deprivation responses. *Genetics* **181:** 889-905.
3. Wu P, Ma L, Hou X, Wang M, Wu Y, Liu F, Deng XW. 2003. Phosphate starvation triggers distinct alterations of genome expression in *Arabidopsis* roots and leaves. *Plant Physiol.* **132:** 1260-1271.
4. Yehudai-Resheff S, Zimmer SL, Komine Y, Stern DB. 2007. Integration of chloroplast nucleic acid metabolism into the phosphate deprivation response in *Chlamydomonas reinhardtii*. *Plant Cell* **19:** 1023-1038.
5. Hammond JP, Broadley MR, White PJ. 2004. Genetic responses to phosphorus deficiency. *Ann. Bot.* **94:** 323-332.
6. Wykoff DD, Grossman AR, Weeks DP, Usuda H, Shimogawara K. 1999. Psr1, a nuclear localized protein that regulates phosphorus metabolism in *Chlamydomonas*. *Proc. Natl. Acad. Sci. USA* **96:** 15336-15341.
7. Merchant SS, Prochnik SE, Vallon O, Harris EH, Karpowicz SJ, Witman GB, *et al.* 2007. The *Chlamydomonas* genome reveals the evolution of key animal and plant functions. *Science* **318:** 245-250.
8. Aksoy M, Pootakham W, Grossman AR. 2014. Critical function of a *Chlamydomonas reinhardtii* putative polyphosphate polymerase subunit during nutrient deprivation. *Plant Cell* **26:** 4214-4229.
9. Miller R, Wu G, Deshpande RR, Vieler A, Gärtner K, Li X, *et al.* 2010. Changes in transcript abundance in *Chlamydomonas reinhardtii* following nitrogen deprivation predict diversion of metabolism. *Plant Physiol.* **154:** 1737-1752.
10. Boyle NR, Page MD, Liu B, Blaby IK, Casero D, Kropat J, *et al.* 2012. Three acyltransferases and nitrogen-responsive regulator are implicated in nitrogen starvation-induced triacylglycerol accumulation in *Chlamydomonas*. *J. Biol. Chem.* **287:** 15811-15825.
11. Blaby IK, Glaesener AG, Mettler T, Fitz-Gibbon ST, Gallaher SD, Liu B, *et al.* 2013. Systems-level analysis of nitrogen starvation–induced modifications of carbon metabolism in a *Chlamydomonas reinhardtii* starchless mutant. *Plant Cell* **25:** 4305-4323.
12. González-Ballester D, Casero D, Cokus S, Pellegrini M, Merchant SS, Grossman AR. 2010. RNA-seq analysis of

sulfur-deprived *Chlamydomonas* cells reveals aspects of acclimation critical for cell survival. *Plant Cell* **22:** 2058-2084.
13. Pootakham W, Gonzalez-Ballester D, Grossman AR. 2010. Identification and regulation of plasma membrane sulfate transporters in *Chlamydomonas*. *Plant Physiol.* **153:** 1653-1668.
14. Aksoy M, Pootakham W, Pollock SV, Moseley JL, González-Ballester D, Grossman AR. 2013. Tiered regulation of sulfur deprivation responses in *Chlamydomonas reinhardtii* and identification of an associated regulatory factor. *Plant Physiol.* **162:** 195-211.
15. Moseley JL, Chang C-W, Grossman AR. 2006. Genome-based approaches to understanding phosphorus deprivation responses and PSR1 control in *Chlamydomonas reinhardtii*. *Eukaryot. Cell* **5:** 26-44.
16. Blaby-Haas CE, Merchant SS. 2012. The ins and outs of algal metal transport. *Biochim. Biophys. Acta* **1823:** 1531-1552.
17. Hsieh SI, Castruita M, Malasarn D, Urzica E, Erde J, Page MD, *et al.* 2013. The proteome of copper, iron, zinc, and manganese micronutrient deficiency in *Chlamydomonas reinhardtii*. *Mol. Cell. Proteomics* **12:** 65-86.
18. Page MD, Allen MD, Kropat J, Urzica EI, Karpowicz SJ, Hsieh SI, *et al.* 2012. Fe sparing and Fe recycling contribute to increased superoxide dismutase capacity in iron-starved *Chlamydomonas reinhardtii*. *Plant Cell* **24:** 2649-2665.
19. Bölling C, Fiehn O. 2005. Metabolite profiling of *Chlamydomonas reinhardtii* under nutrient deprivation. *Plant Physiol.* **139:** 1995-2005.
20. Lu N, Chen J-H, Wei D, Chen F, Chen G. 2016. Global metabolic regulation of the snow alga *Chlamydomonas nivalis* in response to nitrate or phosphate deprivation by a metabolome profile analysis. *Int. J. Mol. Sci.* **17:** 694.
21. Lee J-E, Cho YU, Kim KH, Lee DY. 2016. Distinctive metabolomic responses of *Chlamydomonas reinhardtii* to the chemical elicitation by methyl jasmonate and salicylic acid. *Process Biochem.* **51:** 1147-1154.
22. Lee DY, Fiehn O. 2008. High quality metabolomic data for *Chlamydomonas reinhardtii*. *Plant Methods* **4:** 1.
23. Lee DY, Fiehn O. 2013. Metabolomic response of *Chlamydomonas reinhardtii* to the inhibition of target of rapamycin (TOR) by rapamycin. *J. Microbiol. Biotechnol.* **23:** 923-931.
24. Lee DY, Park J-J, Barupal DK, Fiehn O. 2012. System response of metabolic networks in *Chlamydomonas reinhardtii* to total available ammonium. *Mol. Cell. Proteomics* **11:** 973-988.
25. Scholz M, Fiehn O. 2007. SetupX – a public study design database for metabolomic projects, pp. 169-180. *In* Altman RB, Dunker AK, Hunter L, Murray T, Klein TE (eds.). *Proceedings of the Pacific Symposium on Biocomputing*, Grand Wailea, Maui, Hawaii, 3-7 January 2007. World Scientific Publishing, Singapore.
26. Xia J, Sinelnikov IV, Han B, Wishart DS. 2015. MetaboAnalyst 3.0 – making metabolomics more meaningful. *Nucleic Acids Res.* **43:** W251-W257.
27. Huang CY, Roessner U, Eickmeier I, Genc Y, Callahan DL, Shirley N, *et al.* 2008. Metabolite profiling reveals distinct changes in carbon and nitrogen metabolism in phosphate-deficient barley plants (*Hordeum vulgare* L.). *Plant Cell Physiol.* **49:** 691-703.
28. Schlüter U, Colmsee C, Scholz U, Bräutigam A, Weber AP, Zellerhoff N, *et al.* 2013. Adaptation of maize source leaf metabolism to stress related disturbances in carbon, nitrogen and phosphorus balance. *BMC Genomics* **14:** 442.
29. Khozin-Goldberg I, Cohen Z. 2006. The effect of phosphate starvation on the lipid and fatty acid composition of the fresh water eustigmatophyte *Monodus subterraneus*. *Phytochemistry* **67:** 696-701.
30. Feng T-Y, Yang Z-K, Zheng J-W, Xie Y, Li D-W, Murugan SB, *et al.* 2015. Examination of metabolic responses to phosphorus limitation via proteomic analyses in the marine diatom *Phaeodactylum tricornutum*. *Sci. Rep.* **5:** 10373.
31. Smilde AK, Jansen JJ, Hoefsloot HC, Lamers R-JA, Van Der Greef J, Timmerman ME. 2005. ANOVA-simultaneous component analysis (ASCA): a new tool for analyzing designed metabolomics data. *Bioinformatics* **21:** 3043-3048.
32. Lee DY, Heo S, Kim SG, Choi H-K, Lee H-J, Cho S-M, Auh J-H. 2013. Metabolomic characterization of the region-and maturity-specificity of *Rubus coreanus* Miquel (*Bokbunja*). *Food Res. Int.* **54:** 508-515.
33. Wiklund S, Johansson E, Sjoestroem L, Mellerowicz EJ, Edlund U, Shockcor JP, *et al.* 2008. Visualization of GC/TOF-MS-based metabolomics data for identification of biochemically interesting compounds using OPLS class models. *Anal. Chem.* **80:** 115-122.
34. Park SJ, Jeong IH, Kong BS, Lee J-E, Kim KH, Lee DY, Kim HJ. 2016. Disease type- and status-specific alteration of *csf* metabolome coordinated with clinical parameters in inflammatory demyelinating diseases of CNS. *PLoS One* **11:** e0166277.
35. Mothes K, Schütte H. 1963. The biosynthesis of alkaloids II. *Angew. Chem. Int. Ed. Engl.* **2:** 441-458.
36. Dewick PM. 2009. The shikimate pathway: aromatic amino acids and phenylpropanoids, pp. 137-186. *Medicinal Natural Products: A Biosynthetic Approach.* 3rd Ed. John Wiley & Sons, NY. USA.